The open membrane database: Synthesis–structure–performance relationships of reverse osmosis membranes

Cody L. Ritt [a,1], Timothée Stassin [b,1], Douglas M. Davenport [b], Ryan M. DuChanois [a], Ines Nulens [b], Zhe Yang [c], Adi Ben-Zvi [d], Naama Segev-Mark [d], Menachem Elimelech [a], Chuyang Y. Tang [c], Guy Z. Ramon [d], Ivo F.J. Vankelecom [b], Rhea Verbeke [b,*]

[a] Department of Chemical and Environmental Engineering, Yale University, New Haven, CT, 06520-8286, USA
[b] Centre for Membrane Separations, Adsorption, Catalysis and Spectroscopy for Sustainable Solutions (cMACS), KU Leuven, Celestijnenlaan 200F Box 2454, 3001, Leuven, Belgium
[c] Department of Civil Engineering, The University of Hong Kong, Pokfulam Road, Hong Kong, SAR, PR China
[d] Department of Civil and Environmental Engineering, Technion—Israel Institute of Technology, Haifa, 3200003, Israel

ABSTRACT

Since the advent of thin-film composite polyamide membranes brought forth a breakthrough in desalination and water purification membranes nearly half a century ago, recent years have only witnessed marginal improvements in the water-salt selectivity of these membranes. The slow progression is partly attributable to limited understanding of membrane synthesis–structure–performance relationships. A centralized archive of reverse osmosis membrane (RO) characterization data may lead to a shared understanding of features that maximize RO performance and unify research efforts. The Open Membrane Database (OMD), which can be found at www.openmembranedatabase.org, is a growing database of over 600 water purification and desalination membranes that are sourced from peer-reviewed journals, patents, and commercial product data. Here, we outline the detailed functionality of the database, the transport theory underlying the membrane performance calculations, and best practices for membrane performance testing and reporting. The user-sourced, open-access database may be used to benchmark novel RO membranes against the state of the art, conduct meta-analyses, and develop synthesis–structure–performance relationships, each of which will be critical to advancing membrane development.

1. Introduction

Securing equitable access to safe drinking water around the globe remains one of the most daunting challenges of this century [1]. Pressures on water resources are rapidly mounting from population growth, industrialization, and climate change [2]. While water conservation will be critical in preserving water resources, the desalination of seawater and other saline sources (e.g., brackish groundwater and wastewater effluent) has also been highlighted as a necessary strategy for curtailing global water scarcity [3–5]. Pressure-driven reverse osmosis (RO) is the predominant desalination process [6], being the most widely employed primarily due to its low energy consumption and cost relative to other technologies [4].

Seawater RO is a mature technology. Initial investigations into its use began in 1949 before advancements in membrane structure finally made the technology practical over a decade later [7,8]. The following 30 years witnessed an evolution in seawater RO as new membrane materials and fabrication techniques emerged. This period of exploration led to the development of thin-film composite (TFC) membranes made from fully aromatic crosslinked polyamide, which remain the state of the art to this day [9]. Despite the effectiveness and widespread use of TFC polyamide membranes, their propensity to foul [10], poor resistance to oxidants (e.g., chlorine) [11], and inadequate water-salt selectivity for certain water treatment processes [12–14] leaves room for improvement. Consequently, RO membrane research has experienced a renaissance over the past decade as researchers explore new avenues to overcome the limitations of polyamide (Fig. 1A).

Membranes offering both high water permeability and high water-

---

* Corresponding author.
E-mail address: rhea.verbeke@kuleuven.be (R. Verbeke).
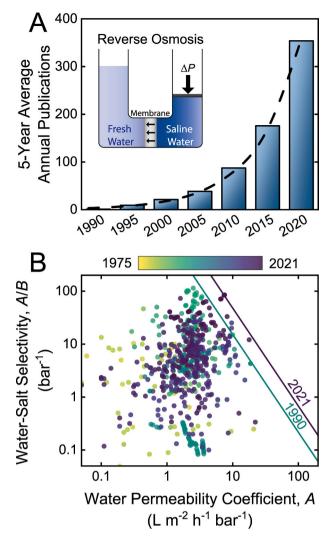[1] These authors contributed equally to this work.

Fig. 1. Evolution of reverse osmosis (RO) membranes. (A) Average number of publications on RO desalination membranes over a five-year span from 1990 to 2020. Annual publications were quantified on Web of Science™ under the following search criteria: membrane, desalination, and reverse osmosis, while excluding the topics distillation, pervaporation, electrodialysis, and forward osmosis. (B) Water-salt selectivity, A/B, with respect to the water permeability coefficient, A, for RO membranes. Membranes are color-mapped by their report year, spanning the years 1975–2021. Membranes were sourced from the Open Membrane Database on August 1st, 2021. (For interpretation of the references to color in this figure legend, the reader is referred to the Web version of this article.)

salt selectivity are ideal for separations processes, with recent analyses indicating the latter is exceptionally more important [15,16]. However, a trade-off between permeability and selectivity, which is ubiquitous among separation materials, limits the achievable water-salt selectivity of seawater RO membranes to permeabilities in the range ~1–3 L m^{-2} h^{-1} bar^{-1} [15,17]. Despite recent efforts to advance RO membranes (Fig. 1A), their performance has only improved marginally since 1990 (Fig. 1B). This is, in large part, the result of membrane innovation and design being constrained to empirical approaches, as membranes with sub-nm pores (i.e., free-volume elements) are still considered 'black boxes' due to knowledge gaps surrounding molecular-level transport across the dense polymer film [18]. Novel materials and fabrication techniques that are critically needed to overcome current performance limitations necessitate improved membrane synthesis–structure–performance relationships [9,19].

The solution-diffusion model is conventionally used to describe

macroscopic transport observations with two simplified phenomenological permeability coefficients [20]. The water (A) and salt (B) permeability coefficients, or permeances, describe the permeation rate of these species across the membrane under a given driving force (i.e., transmembrane pressure difference or concentration difference). The ratio of these two coefficients (A/B) is commonly used to describe the water-salt selectivity of the membrane. Permeability-selectivity trade-off curves can be constructed by comparing A/B against A for a collection or series of membranes. Systematically studying changes in these values with respect to synthesis conditions or membrane modifications, such as curing time during fabrication or chlorine treatment [21–23], respectively, is frequently employed to develop synthesis–structure–performance relationships for various materials. Additionally, periodic compilations of performance data from previous works or commercial sources are published to inform the current state of RO membrane efficacy [9,15,17,24].

To date, the membrane community has leaned on these periodically published permeability-selectivity trade-off curves to direct innovation. This feedback loop has provided important guidance to the field. Nonetheless, the current approach has several limitations. Publications are static in nature; thus, the periodicity of these reports captures only a snapshot of the status quo in membrane science. Furthermore, the characterization and analysis of performance data, such as the consideration of concentration polarization (CP) when estimating A and B values, is variable among reports. Data accessibility also presents a prominent issue. Although existing in a digitally connected world, many scientific fields are experiencing a data sharing crisis [25], with funding agencies enforcing increasingly stringent policies on open access to research data [26]. Published data are rarely shared on public repositories and instead typically require personal requests sent to the author—an unreliable, time-consuming, and often ineffective method [27]. Even when successfully obtained, salient properties of the dataset that are crucial for meta-analyses are not always included [25].

We look to draw upon the successes of gas separations [28], crystallography [29], structural biology [30], and others who have developed open-access databases for the collection and dissemination of relevant data to advance their respective fields. Here, we detail the extensive data curation central to forming the Open Membrane Database (OMD)—a growing database of over 600 desalination and water purification membranes that are sourced from peer-reviewed journals, patents, and commercial product data. The initial release of the OMD focuses on the performance characteristics (i.e., A and B values) and physicochemical properties of RO membranes. We outline the detailed functionality of the OMD, the transport theory underlying the membrane performance calculations, and best practices for membrane performance testing and reporting. The OMD offers several advantages over the current status quo for studying synthesis–structure–performance relationships (Table 1) that will facilitate future research and accelerate

Table 1
Comparison of data features in periodically published compilations of performance data (status quo) and the OMD.

Data Features	Status Quo	OMD
Update Frequency[a]	~1–2 years	Real time
Sourcing[b]	Limited scope	Entire field
Processing[c]	Variable	Uniform and transparent
Exploration[d]	None	Interactive
Accessibility[e]	Available upon request	Open access to raw data

Note.
[a] Refers to the rate at which new data are added to the dataset for comparison.
[b] Refers to the sources from which data are collected.
[c] Refers to the analysis and characterization of raw data from literature for reporting performance characteristics.
[d] Refers to the ability for users to manipulate the dataset for targeted discovery (e.g., filtering by membrane chemistry).
[e] Refers to the availability of the presented data for advanced exploration.

discovery [25,31]. In particular, the user-sourced open-access database offers a transparent platform to benchmark novel membranes, conduct meta-analyses, and develop synthesis–structure–performance relationships with uniform reporting. Such a database elicits substantial promise for advancing the development of desalination and water purification membranes.

2. Data sourcing

2.1. Data origins and constraints

The OMD comprises data compiled from technical datasheets (i.e., commercial sources), patents, and peer-reviewed scientific reports to provide a comprehensive assessment of the field. We publish all relevant membranes rather than only those that perform best. This approach produces a large dataset that contains information critical for conducting instructive meta-analyses.

Only RO membranes are being included in the initial release of the OMD. For the purposes of the OMD, we define RO membranes as membranes that can achieve real (intrinsic) sodium chloride (NaCl) rejection (R_{NaCl}) ≥80%. We consider membranes operating below this separation efficacy (i.e., $R_{NaCl} < 80\%$) to be nanofiltration (NF) membranes. The similar, and often overlapping, range in pore sizes of RO and NF membranes can result in performances that are difficult to distinguish [9,32]. Our selection follows the guidance of commercial sources [33], although previous reports have instead designated this cut-off as 90% NaCl rejection [24,34]. We therefore note that this cut-off is not intended to be prescriptive beyond the purposes of the OMD.

While only RO membranes are currently included in the OMD, some exceptions exist for membranes that are part of a series. We refer to a series as a set of membranes from a single source (e.g., publication) of similar nature that were modified by varying treatments, usually with respect to a control. Membranes in a series with $R_{NaCl} < 80\%$ are included in the database if one or more of the membranes in the entire series achieves RO-level performance (i.e., $R_{NaCl} \geq 80\%$). This protocol is important for maintaining the intellectual integrity of the studies included in the database. For example, within the OMD, we include a polyamide membrane prepared by molecular layer-by-layer (mLbL) deposition with $R_{NaCl} = 77.4\%$ [35]. This study reported improvement in the salt separation efficacy of the membrane by increasing the number of trilayers deposited, eventually achieving $R_{NaCl} = 91.4\%$ with six trilayers. In such a case, the poorly performing membrane may represent a key datapoint for larger analyses, potentially informing the critical thickness of membranes prepared via mLbL deposition.

Membranes applied to non-RO processes, such as forward osmosis (FO), but characterized in RO mode, are also included. RO mode means that the driving force applied across the membrane to desalinate water is hydraulic pressure rather than osmotic pressure generated from a draw solution. FO has been extensively studied over the last two decades as an emerging desalination and water treatment technology [36,37]. Although a distinct technology from RO, the overarching goals remain the same for both technologies: achieve high water-solute selectivity and high water permeability. However, the membrane properties that influence selectivity and permeability differ between RO and FO [15]. For example, the structural parameter (S), which describes the support layer, is critically important for maximizing water flux in FO [36], but in RO, active layer properties predominantly influence water flux [15]. The design approach for FO membranes is thus atypical for RO and may produce poor performing RO membranes. Nevertheless, a collection of data possessing a wide range of variables and performances can improve the effect size (i.e., a measure of the strength of a relationship between two variables [38]) in meta-analyses [39].

2.2. Collected membrane and testing information

Details of the reporting source, synthesis, experimental conditions,

physical characteristics, and performance are collected and reviewed for each membrane submitted to the OMD (Table S1). To account for variability in reporting, the inclusion of less critical information (e.g., contact angle) is optional. A global identifier must be used for the reporting source. Peer-reviewed scientific reports and patents are identified by their digital object identifier (DOI) and patent number, respectively. Commercial sources do not have rigid identifiers for their membranes; we thus identify them by the web address of the technical datasheet. The report title, year of publication or revision, and the last name of the first author are also included during submission.

We classify membranes by the structure and chemistry of their selective layer, as well as modifications applied to the membrane during or after synthesis. Common membrane structures are asymmetric, TFC, thin-film nanocomposite (TFN), or inorganic (Fig. 2). Asymmetric membranes are anisotropic structures that transition from a dense and selective skin layer down to a porous substructure, as typically prepared

Asymmetric

Thin-film composite (TFC)

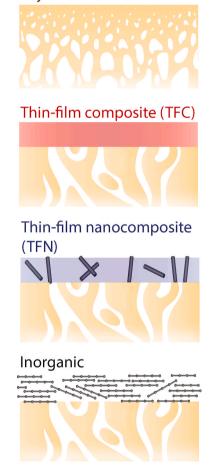**Thin-film nanocomposite (TFN)**

Inorganic

Fig. 2. Schematic representation of four membrane structures relevant to RO: Asymmetric membranes with a dense skin layer (top); thin-film composite (TFC) membrane, where the dense polymer layer, or 'selective layer,' is marked in red atop a porous support (upper middle); thin-film nanocomposite (TFN), or hybrid, membrane illustrating the addition of carbon nanotubes to the polymer selective layer, marked in blue, atop a porous support (lower middle); inorganic membranes where the inorganic selective layer is exemplified by a graphitic laminate structure atop a porous support (bottom). Although depicting a composite structure for the inorganic membrane, we note that support layers are not required for inorganic membranes, as inorganic membranes can be support-free or take on other structures (e.g., asymmetric). In all cases, the membrane structure is classified by the nature of the selective layer. The selective layers illustrated here are not drawn to scale. (For interpretation of the references to color in this figure legend, the reader is referred to the Web version of this article.)

via the process of phase inversion [40]. TFC membranes consist of a thin, dense polymer layer deposited on top of a porous support. TFN, or 'hybrid,' membranes are more loosely defined. They are similar to TFC membranes but with the addition of a nanomaterial, such as carbon nanotubes or silver nanoparticles, to the selective layer [41,42]. Inorganic membranes define any membrane where the selective layer is composed of primarily inorganic materials, such as graphene oxide laminate structures. We define the chemistry of the membrane as the predominant material by which the selective layer is composed. For example, thin-film polyamide membranes with nanoparticles embedded in the selective layer are classified as TFN structures having polyamide chemistry. We do not consider nanoparticles embedded in the support layer as TFNs; rather, this is a modification to the support layer during TFN synthesis. Other common membrane modifications, such as solvent annealing, are listed in Table S2.

Experimental conditions, such as salt concentration, solution pH, applied hydraulic pressure, and CP modulus are critical to membrane performance [43]. These conditions vary in many reports and can influence membrane ionization and swelling behavior [44,45], compaction [46,47], and transport modeling [48,49]. It is strongly encouraged to follow industry standard testing conditions for RO membranes (Table S3) to avoid disparities in reporting that originate from the operational conditions. For instance, coupon-scale membrane experiments should be operated under cross-flow hydrodynamics to mimic industrial conditions [50–52]. However, the challenges associated with fabricating robust bench-scale membrane systems that operate at industrially relevant hydraulic pressures under cross-flow has resulted in the widespread use of dead-end filtration cells [52,53]. We therefore accept membranes characterized under operating conditions outside of the industrial standards. Including these critical experimental details is required for submission to the OMD, in addition to the filtration mode (i. e., dead-end vs. cross-flow) and estimated osmotic pressure. The presence of solutes other than NaCl in solution is also documented, as mixed-feed solutions can influence the overall mass transfer [54].

Membrane performance is inextricably linked to the physical characteristics of the membrane. The *A* and *B* coefficients are inversely proportional to the selective layer thickness [55] and are variably affected by the roughness and hydrophilicity of the selective layer. Roughness is most noteworthy for its impact on membrane fouling; however, the structure and degree of roughness can greatly influence membrane permeability [56–58]. The hydrophilicity of the selective layer is approximated by its measured contact angle with water [59]. More hydrophilic surfaces typically increase water uptake, leading to increased water permeability [47,55]. In general, greater water sorption coincides with higher salt sorption, which produces a permeability-selectivity trade-off [17]. These characteristics, albeit of notable importance, are optionally included in the OMD due to the low reporting frequency in published works.

The salient properties and operating parameters noted above govern the overall membrane performance (Fig. 3). When provided in the source data, the OMD directly collects and reports *A* and *B* coefficients for published membranes, without any alteration or re-computation, regardless of the availability of details or assumptions made when calculating the CP modulus (e.g., neglection of CP). This is intended to maintain the intellectual integrity of the report. The OMD distinguishes whether details on the calculation of the CP modulus are provided in the original report (i.e., as reported) or not (i.e., not available).

Often, the permeability and selectivity of the membrane are instead reported in terms of water flux (J_W) and observed rejection (R_{obs}). These properties are operationally dependent, however, and therefore cannot be used to compare the performance of membranes tested under different operating conditions. In cases where *A* and *B* are not directly reported, J_W and R_{obs} values are translated into *A* and *B* coefficients by accounting for CP in the diffusive boundary layer at the feed channel-membrane interface (details in Section 3). In all cases, error bars are not collected in the OMD as the reporting of error bars is not
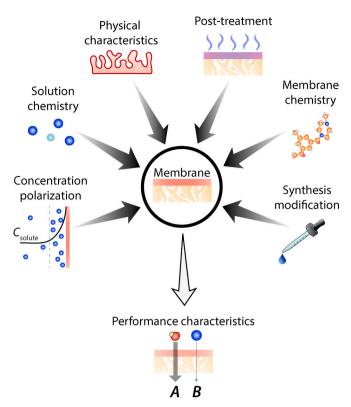

Fig. 3. Schematic illustration of various membrane properties, treatments, and process conditions collected by the Open Membrane Database (OMD) that influence membrane performance characteristics, such as water and salt permeability coefficients (*A* and *B*, respectively). From left to right of the schematic these include: concentration polarization (e.g., fluid dynamics), solution chemistry (e.g., pH), physical characteristics (e.g., roughness), post-treatment (e.g., solvent annealing), membrane chemistry (e.g., polymer chemistry), and synthesis modification (e.g., dopants).

standardized in literature. For instance, error bars could represent one standard deviation of uncertainty, one standard error, or a particular confidence interval. Assuming their representation could propagate additional error.

3. Transport theory

3.1. Calculating A and B coefficients

The water permeability coefficient, *A*, can be determined by its relation to water flux, J_W. The water flux across the membrane is described by the solution-diffusion model as [20,60].

$$J_W = A(\Delta P - \Delta \pi_m) \tag{1}$$

where ΔP is the applied hydraulic pressure and $\Delta \pi_m$ is the osmotic pressure difference across the membrane active layer between the feed and permeate sides. Osmotic pressure is the pressure that would need to be applied to prohibit a pure solvent from passing through a semipermeable barrier into a given solution by osmosis [61]. Osmotic pressure was calculated using the OLI activity coefficient model (OLI Systems, Morris Plains, NJ) for membranes uploaded to the OMD prior to initial release. The osmotic pressure of a solution depends on the concentration of dissolved salts and can be calculated from empirical correlation equations (e.g., Eq. 3b in Ref. [62]) or the modified van't Hoff equation [60]:

$$\pi = n \Phi_c R_g T C \tag{2}$$

where *n* is the number of dissociable species (e.g., two for NaCl), Φ_c is

the osmotic coefficient [63], R_g is the ideal gas constant, T is the absolute temperature, and C is the molar concentration. Correlation equations are often preferred to calculate osmotic pressure due to greater accuracy at high salinities compared to the van't Hoff equation [64].

The osmotic pressure at the membrane surface is higher than the bulk feed due to the influence of CP (i.e., $\Delta\pi_m > \Delta\pi_f$). Eq. (1) can be modified using film theory to account for CP effects [60]:

$$J_W = A\left[\Delta P - \Delta\pi_f \exp\left(\frac{J_W}{k_f}\right)\right] \tag{3}$$

where $\Delta\pi_f$ is the osmotic pressure difference between the feed and permeate solutions and k_f is the overall feed-side mass transfer coefficient averaged for all feed solutes. More details on calculating k_f will be provided in Section 3.2.

The A coefficient is readily determined by measuring J_W with deionized water, eliminating osmotic pressure effects. In this case, A is commonly termed the 'pure water permeability coefficient.' However, solution chemistry can induce physicochemical changes to the membrane, such as salt-induced de-swelling of the selective layer [45], that are not captured in pure water filtration experiments. Changes in selective layer swelling influence the overall thickness of the film and can be critical to the resulting A coefficient [44].

The B coefficient reflects the separation capacity of the membrane paired with its permeability. Salt separation is commonly reported by the observed rejection, R_{obs},

$$R_{obs} = \left(1 - \frac{C_p}{C_f}\right) \tag{4}$$

where C_p and C_f denote the salt concentration in the permeate and feed solution, respectively. Using the salt concentration measured in the permeate, the salt flux, J_S, is given by

$$J_S = J_W C_p \tag{5}$$

Salt flux is modeled by Fickian diffusion to generate the B coefficient:

$$B = \frac{J_S}{\Delta C_m} = \frac{J_S}{\Delta C_f \exp\left(\frac{J_W}{k_{sol}}\right)} \tag{6}$$

where ΔC_m is the salt concentration difference across the membrane selective layer, ΔC_f is the concentration difference between the feed and permeate solutions, and k_{sol} is the feed-side mass transfer coefficient for the solute of interest. Film theory can again be applied to relate ΔC_m to ΔC_f by accounting for CP effects. When measuring the salt flux of single-salt solutions, k_f and k_{sol} are analogous. If unreported, k_f and k_{sol} were both estimated as 100 L m^{-2} h^{-1} [15] for membrane data uploaded to the OMD from previously published reports.

We note that assuming k_f can lead to some error in the computed A and B coefficients. The extent of the error remains unknown and warrants future investigation beyond the current scope of this work. Despite the uncertainty inherent to the assumptions, we posit that CP-based assumptions are necessary for comparing performance characteristics of RO membranes. Less than 5% of the 651 membranes included in the OMD at launch were associated with reported CP moduli or k_f in their original documents. The lack of CP moduli reporting in membrane literature is evidently extensive and has led to the neglect of CP effects in recent meta-analyses of membrane performance [24]. Consequently, ref. [24] underpredicts the performance of the membranes investigated to varying extents.

Real rejection (R_{real}) is the intrinsic separation efficacy of the membrane. It differs from R_{obs} in that it considers CP effects (i.e., $R_{real} = 1 - C_p/C_m$). R_{real} can be modeled as a function of the membrane's water-salt selectivity, A/B [15,55]:

$$R_{real} = \frac{\frac{A}{B}(\Delta P - \Delta\pi_m)}{1 + \frac{A}{B}(\Delta P - \Delta\pi_m)} \tag{7}$$

Water-salt selectivity can be further extended to the water-salt permselectivity (P_W/P_S) for membranes that do not swell excessively and are not exposed to relatively high pressures [55,65]:

$$\frac{P_W}{P_S} = \left(\frac{A}{B}\right)\left(\frac{R_g T}{V_W}\right) \tag{8}$$

where V_W is the molar volume of water. P_W/P_S is the ratio of the diffusive water permeability (P_W) to the diffusive salt permeability (P_S) and is a material property that describes the intrinsic selectivity of the membrane. The diffusive water and salt permeabilities are obtained by normalizing the A and B coefficients to the selective layer thickness (δ): $P_W = A\delta$ and $P_S = B\delta$.

P_W and P_S are reported in the OMD based on the availability of thickness data for selective layers. However, we note that exact thickness measurements of the selective layer are often unreliable due to inadequate measurement techniques at these length scales, or even conceptually impossible due to diffuse transitions from the selective layer to the support layer at the molecular level. Determining the diffusion thickness is further challenged by nanoscopic voids contained in selective layer structures that can be very rough or tortuous relative to their overall thickness [66–68]. Roughness is especially prevalent for TFC polyamide membranes [24], which possess the well-known ridge-and-valley structure.

3.2. Estimating concentration polarization (CP) modulus

CP is the accumulation of rejected solutes near the membrane surface that results in the formation of a 'polarized layer.' This phenomenon increases the osmotic pressure at the membrane surface, reducing the water flux due to a decreased effective driving force across the membrane at a fixed hydraulic pressure. The effect of CP on membrane performance, as mentioned in Section 3.1, can be approximated with film theory [60]:

$$\frac{C_m}{C_f} = (1 - R_{obs}) + R_{obs} \exp\left(\frac{J_W}{k_f}\right) \tag{9}$$

where C_m/C_f is the CP modulus, the ratio of the solute concentration at the membrane surface to that of the bulk feed solution. If no CP exists, the CP modulus is unity. This situation only occurs when the membrane does not reject the target solute or J_W/k_f approaches zero. The latter case generally pertains to membranes operated at low flux, which is common for commercial RO operation but may not hold for bench-scale operation [69].

The feed-side mass transfer coefficient, k_f, is an important component in the CP modulus, as displayed in Eq. (9). Hence, appropriate estimations of k_f are necessary to accurately report membrane performance data [70]. Values for k_f can be estimated experimentally by the osmotic pressure or velocity variation methods [71], or k_f can be calculated from the dimensionless Sherwood number (Sh) [71,72]:

$$k_f = \frac{ShD}{D_h} = a Re^b Sc^c \tag{10}$$

where D is the solute diffusion coefficient, D_h is the hydraulic diameter of the cell, Re is the dimensionless Reynolds number, Sc is the dimensionless Schmidt number, and a, b, c are adjustable dimensionless parameters that change based on system geometry and laminar or turbulent conditions [73]. The diffusivity of NaCl in water at 25 °C varies non-linearly with concentration between roughly 1.47×10^{-5} and 1.62×10^{-5} cm^2 s^{-1} [74]. An overview of the most used Sh equations defined for laminar and turbulent conditions in cross-flow and stirred cell (i.e., dead-end filtration) conditions is reported elsewhere

[70].

4. Database content and functionalities

4.1. Open Membrane Database (OMD) content

The OMD is a continually growing database, which currently has more than 600 RO membranes listed for public use. Membrane data are sourced from previously published scientific reports, patents, and commercial datasheets. As of this writing, RO membrane data in the OMD is sourced primarily from peer-reviewed scientific reports (63%), whereas patents and commercial datasheets make up roughly 29% and 8% of the membranes in the database, respectively (Fig. 4). Data are sourced from reports from 1975 to the most recent publications and releases.

Meeting current and future global demands for improved water treatment necessitates an interdisciplinary approach. Various scientific disciplines have converged upon membrane-based separation processes to tackle some of these challenges. However, introducing disciplines with ranging backgrounds to membrane technologies has presented difficulties. Incorrect interpretation of physical phenomena observed during membrane experimentation [75,76] as well as improper performance calculations [77,78] have pervaded scientific literature. The OMD aims to unify the broader public investigating membrane technologies by providing discussion and resources for the fundamental principles of membrane-based liquid separations. More importantly, we aim to standardize the calculation (see Eq. (1) – (10)) and reporting of RO membrane performance data with consideration of CP. Calculators for performance characteristics, CP modulus, and osmotic pressure will be provided on the database site. Additionally, we provide common unit converters relevant to membrane processes (Table S4) to reflect the varying metrics used in the global membrane community.

4.2. User access and data processing interface

The OMD is an open-access domain that can be found online at www. openmembranedatabase.org. Use of the OMD is free of charge and does not require any form of registration. A foundational goal of the OMD is to be a sustainable and fully crowd-sourced platform for membrane science. We thus encourage researchers to upload their latest results to supply the OMD with t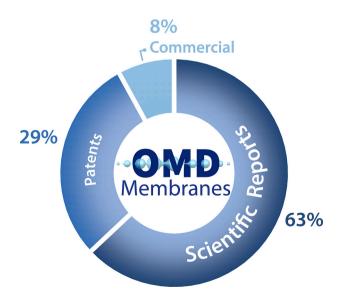he most recent scientific discoveries. Notably, the OMD is not interested in only the best performing membranes that compete with current state-of-the-art RO membranes. The database, and the membrane community, can greatly benefit from the inclusion of membranes spanning a wide range of performance. The submission form guides authors through a step-by-step submission process to collect all relevant membrane information (see Section 2.2). We note that submissions are only allowed for research published in a peer-reviewed journal, possessing a valid DOI. This is to prevent the inclusion of erroneous, biased, or misleading data in the database.

The interactive chart and search functionalities featured on the OMD website allow easy data exploration (Fig. 5). Performance data for membranes with a wide array of physicochemical properties and synthesis conditions can be compared for in-depth analyses. The chart *x*-axis is fixed to the *A* coefficient. The chart *y*-axis can be toggled between different performance metrics, namely A/B, R_{real}, or R_{obs}. The scaling of the axes can also be adjusted between log-normal and linear. Selective layer chemistry, membrane structure, and report year are categories by which the data can be sorted in a legend. These categories provide a glimpse of membrane evolution since the 1970s and demonstrate how most research efforts have shifted toward TFC polyamide membranes.

Beyond chart manipulation, the database can be sorted by as many as 17 different filters. This feature allows researchers to rapidly narrow their search to only the most relevant membranes. Other chart interactions, such as zoom, pan, and selection features also help with narrowing or focusing the chart to data of interest. Once narrowed, datapoints can be individually highlighted in a call-out that depicts the name, year, *A* coefficient, selectivity (A/B, R_{real}, or R_{obs}), and chemistry of the membrane, as depicted in Fig. 5. Multiple datapoints can be highlighted at once if close together. The chart can be exported as a figure file to capture a visual of the selected dataset.

All filtered or selected data appear in a tabulated view below the output chart (Fig. 5). This table contains all information for the selected membranes and their corresponding reports archived in the OMD. All information in the output table can be exported as a text file for further processing and use. Similar to the output chart, this table can be filtered to include only information relevant to the user for data export. Unfilled fields in the output data indicate information that were either unavailable in the membrane report or inapplicable to the membrane. Analyses of data obtained from the OMD are at the discretion of the individual user. Nevertheless, we encourage that data comparisons be conducted with careful consideration of the data source. Despite considering CP effects, comparing data obtained from large module-scale systems (i.e., commercial sources) to small bench-scale systems (i.e., scientific reports and patents) can be tenuous.

We strive to provide the membrane community with the most accurate data and information for membranes uploaded to the OMD. Nevertheless, human error is inevitable for a dataset of this magnitude. User submissions are delayed prior to publication on the database site to allow for review by the OMD team. Details regarding the review process can be found in Fig. S1. We also encourage users to flag any potential errors in the database to provide additional quality control. Membranes reported to the OMD team that may contain erroneous information can be temporarily removed from the database for further investigation and resolution. Reports over more serious concerns, such as membranes submitted from sources with incorrect or misleading performance calculations, will be handled on a case-by-case basis, possibly resulting in permanent removal from the database.

5. Conclusion and outlook

The creation of the OMD presents a potential paradigm shift in how the membrane community shares experimental results. This open-access database establishes a dynamic environment for comparing membrane performance data to understand synthesis–structure–performance relationships under transparent and uniform reporting conditions as detailed in Section 3. Easily accessible data, which include salient
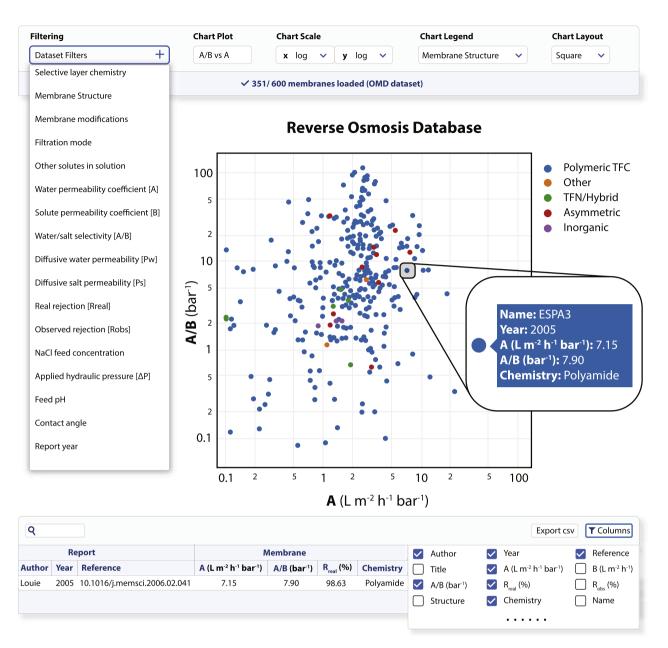

Fig. 4. Membrane representation in the Open Membrane Database (OMD), collected on August 1, 2021, presented as a percentage breakdown comparing membranes from patents, commercial technical datasheets, and peer-reviewed scientific reports.

Fig. 5. Snapshot of the user interface and the dynamic output chart for data exploration on the Open Membrane Database (OMD) website. The snapshot demonstrates the ability to filter the database by various categories (left). Hovering over a datapoint displays its key features on the output chart as seen in the magnified callout. Selected datapoints appear in a filterable table (bottom) where the user can export desired features. This snapshot of the OMD output plot was slightly modified to conform to journal figure requirements.

membrane properties beyond performance metrics, enable future investigations and meta-analyses that can direct innovation in membrane technologies used for liquid separations.

Simple statistical techniques for data analysis are challenged by extensive datasets comprising a multitude of variables. The application of advanced statistical techniques and machine learning for knowledge discovery have gained interest in recent years, with particular uses aimed at databases containing immense storage of raw data [79]. The artificial intelligence and advanced statistical techniques that define machine learning have also recently been used to deconvolute synthesis–structure–performance relationships in desalination technologies [80]. An extension of such techniques to data provided in the OMD could help identify optimal design paths for improving existing membranes. Perhaps more interestingly, knowledge gained from machine learning models could inform design strategies for novel membrane chemistries

or structures not yet introduced to RO that could lead to a significant step-change in performance for the first time in over 30 years. Albeit interesting, we note that reliably interpreting results from machine learning techniques may also require the support of detailed uncertainty assessments [81]—an important consideration for future investigations.

At the time of this writing, the OMD includes only RO membrane data. This is, in part, due to the maturity of the technology. RO membranes have generally well-defined separation performance that can be readily characterized by the solution-diffusion model across a range of operating conditions. These membranes are therefore ideal for a pilot database. Additionally, the OMD is an optimal platform for developing databases for other commonly used membrane separation technologies, such as NF, FO, electrodialysis (ED), and solvent-resistant NF (SRNF) to name a few. This extension could help expedite the progression of less-developed liquid separation technologies that may have more room to

grow than RO.

Credit authorship contribution statement

Cody L. Ritt: Conceptualization, Methodology, Data curation, Writing – original draft, Writing – review & editing, Visualization, Project administration. **Timothée Stassin:** Conceptualization, Resources, Writing – review & editing, Supervision, Project administration, Funding acquisition. **Douglas M. Davenport:** Methodology, Data curation, Writing – review & editing, Project administration. **Ryan M. DuChanois:** Methodology, Data curation, Writing – review & editing. **Ines Nulens:** Methodology, Data curation, Writing – review & editing. **Zhe Yang:** Data curation, Writing – review & editing. **Adi Ben-Zvi:** Data curation, Writing – review & editing. **Naama Segev-Mark:** Data curation. **Menachem Elimelech:** Supervision, Funding acquisition, Writing – review & editing. **Chuyang Y. Tang:** Supervision, Funding acquisition, Writing – review & editing. **Guy Z. Ramon:** Supervision, Funding acquisition, Writing – review & editing. **Ivo F.J. Vankelecom:** Supervision, Funding acquisition, Writing – review & editing. **Rhea Verbeke:** Conceptualization, Resources, Methodology, Writing – review & editing, Supervision, Project administration, Funding acquisition.

Declaration of competing interest

The authors declare that they have no competing financial interests that could have appeared to influence the work reported in this paper.

Acknowledgements

Appendix A. Supplementary data

Supplementary data to this article can be found online at https://doi.org/10.1016/j.memsci.2021.119927.

References

[1] M. Elimelech, The global challenge for adequate and safe water, J. Water Supply Res. T 55 (2006) 3–10.

[2] P. D`Odorico, et al., The global food-energy-water nexus, Rev. Geophys. 56 (2018) 456–531.

[3] C.Y. Tang, et al., Potable water reuse through advanced membrane technology, Environ. Sci. Technol. 52 (2018) 10215–10223.

[4] M. Elimelech, W.A. Phillip, The future of seawater desalination: energy, technology, and the environment, Science 333 (2011) 712–717.

[5] V.G. Gude, Desalination and water reuse to address global water scarcity, Rev. Environ. Sci. Biotechnol. 16 (2017) 591–609.

[6] E. Jones, et al., The state of desalination and brine production: a global outlook, Sci. Total Environ. 657 (2019) 1343–1356.

[7] J. Glater, The early history of reverse osmosis membrane development, Desalination 117 (1998) 297–309.

[8] K.P. Lee, et al., A review of reverse osmosis membrane materials for desalination—development to date and future potential, J. Membr. Sci. 370 (2011) 1–22.

[9] J.R. Werber, et al., Materials for next-generation desalination and water purification membranes, Nat. Rev. Mater. 1 (2016).

[10] S.P. Nunes, Can fouling in membranes be ever defeated? Curr. Opin. Chem. Eng. 28 (2020) 90–95.

[11] R. Verbeke, et al., Chlorine-resistance of reverse osmosis (RO) polyamide membranes, Prog. Polym. Sci. 72 (2017) 1–15.

[12] S.K. Patel, et al., The relative insignificance of advanced materials in enhancing the energy efficiency of desalination technologies, Energy Environ. Sci. 13 (2020) 1694–1710.

[13] B. Sauvet-Goichon, Ashkelon desalination plant – a successful challenge, Desalination 203 (2007) 75–81.

[14] D.L. Shaffer, et al., Seawater desalination for agriculture by integrated forward and reverse osmosis: improved product water quality for potentially less energy, J. Membr. Sci. 415 (2012) 1–8.

[15] J.R. Werber, et al., The critical need for increased selectivity, not increased water permeability, for desalination membranes, Environ. Sci. Technol. Lett. 3 (2016) 112–120.

[16] D. Cohen-Tanugi, et al., Quantifying the potential of ultra-permeable membranes for water desalination, Energy Environ. Sci. 7 (2014) 1134–1141.

[17] G.M. Geise, et al., Water permeability and water/salt selectivity tradeoff in polymers for desalination, J. Membr. Sci. 369 (2011) 130–138.

[18] S. Mondal, et al., Forefronts in structure-performance models of separation membranes, J. Membr. Sci. 588 (2019) 117166.

[19] S.P. Nunes, Thinking the future of membranes: perspectives for advanced and new membrane materials and manufacturing processes, J. Membr. Sci. 598 (2020) 117761.

[20] J.G. Wijmans, R.W. Baker, The solution-diffusion model: a review, J. Membr. Sci. 107 (1995) 1–21.

[21] N.Y. Yip, M. Elimelech, Performance limiting effects in power generation from salinity gradients by pressure retarded osmosis, Environ. Sci. Technol. 45 (2011) 10273–10282.

[22] E. Immelman, et al., Poly(vinyl alcohol) gel sublayers for reverse-osmosis membranes. 1. Insolubilization by acid-catalyzed dehydration, J. Appl. Polym. Sci. 50 (1993) 1013–1034.

[23] R. Verbeke, et al., Controlled chlorination of polyamide reverse osmosis membranes at real scale for enhanced desalination performance, J. Membr. Sci. 611 (2020) 118400.

[24] Z. Yang, et al., The upper bound of thin-film composite (TFC) polyamide membranes for desalination, J. Membr. Sci. 590 (2019) 117297.

[25] N. Noy, A. Noy, Let go of your data, Nat. Mater. 19 (2020), 128-128.

[26] European Commission, Horizon 2020 Online Manual: Open Access & Data Management, 2020. https://ec.europa.eu/research/participants/docs/h2020-funding-guide/cross-cutting-issues/open-access-dissemination_en.htm. (Accessed 1 August 2021).

[27] C. Arnold, Chasing down the data you need, Science (2014), https://doi.org/10.1126/science.caredit.a1400101.

[28] A.W. Thornton, et al., Membrane Society of Australasia, Polymer Gas Separation Membrane Database, 2018. https://membrane-australasia.org/. (Accessed 1 August 2021).

[29] C.R. Groom, et al., The cambridge structural database, Acta Crystallogr. B 72 (2016) 171–179.

[30] H.M. Berman, et al., The protein data bank, Nucleic Acids Res. 28 (2000) 235–242.

[31] J.J. de Pablo, et al., New frontiers for the materials genome initiative, npj Comput. Mater. 5 (2019) 41.

[32] M. Paul, S.D. Jons, Chemistry and fabrication of polymeric nanofiltration membranes: a review, Polymer 103 (2016) 417–456.

[33] DuPont Water Solutions, Nanofiltration (NF): using pressure-driven separation for high rejection of multivalent ions. https://www.dupont.com/water/technologies/nanofiltration-nf.html, 2021. (Accessed 1 August 2021).

[34] X.L. Lu, M. Elimelech, Fabrication of desalination membranes by interfacial polymerization: history, current efforts, and future directions, Chem. Soc. Rev. 50 (2021) 6290–6307.

[35] S. Rajesh, et al., Nanofiber multilayer membranes with tailored nanochannels prepared by molecular layer-by-layer assembly for high throughput separation, J. Mater. Chem. 5 (2017) 4616–4628.

[36] D.L. Shaffer, et al., Forward osmosis: where are we now? Desalination 356 (2015) 271–284.

[37] C. Klaysom, et al., Forward and pressure retarded osmosis: potential solutions for global challenges in energy and water supply, Chem. Soc. Rev. 42 (2013) 6959–6989.

[38] K. Kelley, K.J. Preacher, On effect size, Physchol. Methods 17 (2012) 137–152.

[39] L.B. Shelby, J.J. Vaske, Understanding meta-analysis: a review of the methodological literature, Leisure Sci. 30 (2008) 96–110.

[40] A.K. Holda, I.F.J. Vankelecom, Understanding and guiding the phase inversion process for synthesis of solvent resistant nanofiltration membranes, J. Appl. Polym. Sci. 132 (2015).

[41] B.H. Jeong, et al., Interfacial polymerization of thin film nanocomposites: a new concept for reverse osmosis membranes, J. Membr. Sci. 294 (2007) 1–7.

[42] M.M. Pendergast, E.M.V. Hoek, A review of water treatment membrane nanotechnologies, Energy Environ. Sci. 4 (2011) 1946–1971.

[43] E.M. Van Wagner, et al., Effect of crossflow testing conditions, including feed pH and continuous feed filtration, on commercial reverse osmosis membrane performance, J. Membr. Sci. 345 (2009) 97–109.

[44] C.L. Ritt, et al., Ionization behavior of nanoporous polyamide membranes, Proc. Natl. Acad. Sci. U.S.A. 117 (2020) 30191–30200.

[45] V. Freger, Swelling and morphology of the skin layer of polyamide composite membranes: an atomic force microscopy study, Environ. Sci. Technol. 38 (2004) 3168–3175.

[46] D.M. Davenport, et al., Thin film composite membrane compaction in high-pressure reverse osmosis, J. Membr. Sci. 610 (2020) 118268.

[47] W.H. Zhang, et al., Graphene oxide membranes with stable porous structure for ultrafast water transport, Nat. Nanotechnol. 16 (2021) 337–343.

[48] L. Song, S. Yu, Concentration polarization in cross-flow reverse osmosis, AlChE J 45 (1999) 921–928.

[49] A. Szymczyk, P. Fievet, Investigating transport properties of nanofiltration membranes by means of a steric, electric and dielectric exclusion model, J. Membr. Sci. 252 (2005) 77–88.

[50] D.E. Wiley, et al., Optimization of membrane module design for brackish water desalination, Desalination 52 (1985) 249–265.

[51] F. Maskan, et al., Optimal design of reverse osmosis module networks, AlChE J 46 (2000) 946–954.

[52] G. Belfort, et al., The behavior of suspensions and macromolecular solutions in cross-flow microfiltration, J. Membr. Sci. 96 (1994) 1–58.

[53] A. Simon, et al., A comparative study between classical stirred and ultrasonically-assisted dead-end ultrafiltration, Ultrason. Sonochem. 7 (2000) 183–186.

[54] A.L. Ahmad, et al., Mathematical modeling of multiple solutes system for reverse osmosis process in palm oil mill effluent (POME) treatment, Chem. Eng. J. 132 (2007) 183–193.

[55] G.M. Geise, et al., Fundamental water and salt transport properties of polymeric materials, Prog. Polym. Sci. 39 (2014) 1–42.

[56] B.S. Lalia, et al., A review on membrane fabrication: structure, properties and performance relationship, Desalination 326 (2013) 77–95.

[57] Z. Tan, et al., Polyamide membranes with nanoscale turing structures for water purification, Science 360 (2018) 518–521.

[58] G.Z. Ramon, E.M.V. Hoek, Transport through composite membranes, part 2: impacts of roughness on permeability and fouling, J. Membr. Sci. 425 (2013) 141–148.

[59] G. Hurwitz, et al., Probing polyamide membrane surface charge, zeta potential, wettability, and hydrophilicity with contact angle measurements, J. Membr. Sci. 349 (2010) 349–357.

[60] R.W. Baker, Membrane Technology and Applications, third ed., John Wiley & Sons, U.K., 2012.

[61] S. Marbach, L. Bocquet, Osmosis, from molecular insights to large-scale applications, Chem. Soc. Rev. 48 (2019) 3102–3144.

[62] T.V. Bartholomew, M.S. Mauter, Computational framework for modeling membrane processes without process and solution property simplifications, J. Membr. Sci. 573 (2019) 682–693.

[63] M.H. Sharqawy, et al., Thermophysical properties of seawater: a review of existing correlations and data, Desalin. Water Treat. 16 (2010) 354–380.

[64] R.A. Robinson, R.H. Stokes, Electrolyte Solutions, Dover Publications, Inc., Mineola, New York, 2002.

[65] D.R. Paul, Relation between hydraulic permeability and diffusion in homogeneous swollen membranes, J. Polym. Sci. B Polym. Phys. 11 (1973) 289–296.

[66] L. Lin, et al., Investigating the void structure of the polyamide active layers of thin-film composite membranes, J. Membr. Sci. 497 (2016) 365–376.

[67] X.X. Song, et al., Confined nanobubbles shape the surface roughness structures of thin film composite polyamide desalination membranes, J. Membr. Sci. 582 (2019) 342–349.

[68] C.L. Ritt, et al., Monte Carlo simulations of framework defects in layered two dimensional nanomaterial desalination membranes: implications for permeability and selectivity, Environ. Sci. Technol. 53 (2019) 6214–6224.

[69] S. Kim, E.M.V. Hoek, Modeling concentration polarization in reverse osmosis processes, Desalination 186 (2005) 111–128.

[70] A. Imbrogno, A.I. Schafer, Comparative study of nanofiltration membrane characterization devices of different dimension and configuration (cross flow and dead end), J. Membr. Sci. 585 (2019) 67–80.

[71] G.B. Van den Berg, et al., Mass-transfer coefficients in cross-flow ultrafiltration, J. Membr. Sci. 47 (1989) 25–51.

[72] A.I. Schäfer, et al., Nanofiltration: Principles and Applications, Elsevier, 2005.

[73] M.C. Porter, Concentration polarization with membrane ultrafiltration, Ind. Eng. Chem. Res. 11 (1972) 234–248.

[74] V. Vitagliano, P.A. Lyons, Diffusion coefficients for aqueous solutions of sodium chloride and barium chloride, J. Am. Chem. Soc. 78 (1956) 1549–1552.

[75] S. Zhao, Osmotic pressure versus swelling pressure: comment on "bifunctional polymer hydrogel layers as forward osmosis draw agents for continuous production of fresh water using solar energy", Environ. Sci. Technol. 48 (2014) 4212–4213.

[76] R.C. Smith, et al., Comment on "experimental energy barriers to transporting anions through nanofiltration membranes", Environ. Sci. Technol. 47 (2013) 8985–8986.

[77] T. Foller, R. Joshi, Comment on precisely tunable ion sieving with an Al_{13}–$Ti_3C_2T_x$ lamellar membrane by controlling interlayer spacing, ACS Nano 15 (2021) 9201–9203.

[78] J. Abraham, et al., Tunable sieving of ions using graphene oxide membranes, Nat. Nanotechnol. 12 (2017) 546–550.

[79] W.J. Frawley, et al., Knowledge discovery in databases: an overview, AI Mag. 13 (1992) 57–70.

[80] S. Al Aani, et al., Can machine language and artificial intelligence revolutionize process automation for water treatment and desalination? Desalination 458 (2019) 84–96.

[81] V. Kuleshov, et al., Accurate uncertainties for deep learning using calibrated regression, Proc. Mach. Learn. Res. 80 (2018) 2796–2804.